

## Liquid drop model and quantum pressure resisting noncompact nuclear geometries

J. Töke and W. U. Schröder

*Department of Chemistry, University of Rochester, Rochester, New York 14627*

(Received 18 December 2001; published 26 March 2002)

The importance of quantum effects for exotic nuclear shapes is discussed. Based on an example of a sheet of nuclear matter of infinite lateral dimensions but finite thickness, it is shown that the quantization of states in momentum space, resulting from the confinement of the nucleonic motion in the conjugate geometrical space, generates a pressure resisting such a confinement and, consequently, restoring forces driving the systems toward compact geometries. In the liquid-drop model, these quantum effects are implicitly included in the surface energy term, via a choice of interaction parameters, an approximation that has been found valid for compact shapes, but has not yet been scrutinized for exotic shapes.

DOI: 10.1103/PhysRevC.65.044319

PACS number(s): 21.65.+f, 21.60.Ev, 25.70.Pq

In recent years, noncompact nuclear geometries of bubbles, tori, and sheets have attracted considerable interest [1–8] in the context of nuclear multifragmentation studies. According to the scenarios considered, [2–8] it has been suggested that nuclear systems may assume transiently exotic shapes, and then undergo a characteristic multifragment decay. One of the prominent cases of noncompact geometries is that of an infinite sheet. This case affords a high degree of computational simplicity in theoretical modeling attempts and still shows enough features common to many exotic geometries to serve as a test ground for the validity of crucial concepts. As an example, it has been claimed [3,4] that sufficiently thin sheets of nuclear matter, formed dynamically during a heavy-ion collision, are subject to a new form of instability driven by the proximity interaction of the opposing surfaces. More recently, the concept of this sheet instability has been applied [8] to assess the stability of Coulomb bubbles, in general, and against a *crispation mode*, in particular. In both these latter cases, [3,4,8], the analysis relies critically on the liquid-drop model (LDM). However, the assumptions of the LDM and, in particular, the various proposed sets of model parameters [9–12] were shown to be valid only for regular nuclear geometries but not for exotic ones. Similarly, Boltzmann-Uehling-Uhlenbeck (BUU) [13] or Landau-Vlasov methods [14], used [2,5–7] in most theoretical discussions of noncompact geometries, are not designed to handle quantum effects resulting from strong spatial constraints associated with such geometries.

Below, the importance of quantum effects for the properties of nuclear matter in noncompact spatial shapes is demonstrated for the case of an infinite sheet. The scope of this study is limited to the calculation of the volume energy of symmetric nuclear matter. It is clear, however, that the surface energy would also be affected by quantum phenomena of the type considered. Therefore, the surface energy needs to be calculated accordingly, before realistic model predictions can be made for the geometries of interest. Also, for the sake of simplicity, the Coulomb energy is disregarded in the present study. Central to the approach used in this work is the notion of *bulk* matter as opposed to *surface* matter. The former is characterized by spatial uniformity in the controlling parameters and, most notably, in the nucleonic momentum distribution, while the latter is characterized by a nucle-

onic momentum distribution that is changing rapidly with the spatial coordinate perpendicular to the surface. Only *bulk* matter is the subject of the present study.

The energy per nucleon of *bulk* matter can be calculated using a formalism similar to that suggested by Seyler and Blanchard [9] and employed successfully in the development of the droplet model [10–12]. This formalism, based on the Thomas-Fermi approximation, was modified here to account approximately for effects of a quantization of the nucleonic momentum component  $p_z$  perpendicular to the  $x$ - $y$  surface plane of the sheet. This quantization is a necessary consequence of the spatial confinement of the nucleonic motion by the geometry of a sheet of a finite thickness  $d$ . As discussed further below, it is necessary to distinguish between the *model* thickness  $d$ , used here to construct the momentum distribution of nucleons, and the physical *matter* thickness  $d_m$  describing the profile of the corresponding spatial distribution of nuclear matter. The former quantity  $d$  represents the width of an idealized (square) confining potential well with infinitely high walls and defines the finite elementary quantum of the perpendicular momentum component  $p_z$

$$\Delta p_z = \frac{h}{2d}. \quad (1)$$

As a result of the above quantization of  $p_z$ , single-nucleon states for *bulk* sheet matter populate discrete, infinitely thin sheets in nucleonic momentum space, located at discrete values of the perpendicular momentum component,  $p_z = k\Delta p_z$ , where  $k$  is any nonzero integer. This type of population is in a clear contrast to the uniform population of the Fermi sphere that is usually assumed in Thomas-Fermi calculations [9–12] modeling nuclear matter. An example of such discrete population of a Fermi sphere (FS) of a radius equal to the Fermi momentum  $p_F$  is depicted in Fig. 1. Note that there is no sheet with  $k=0$ , leaving a relatively large gap between the sheets  $p_z = +\Delta p_z$  and  $p_z = -\Delta p_z$ . It is this gap that accounts for most of the quantum effects discussed below.

The quantization of the perpendicular component of the momentum can be described by introducing a population function  $f(\mathbf{p}, z)$ , defined as the density of nucleonic states in momentum space per unit nuclear volume,

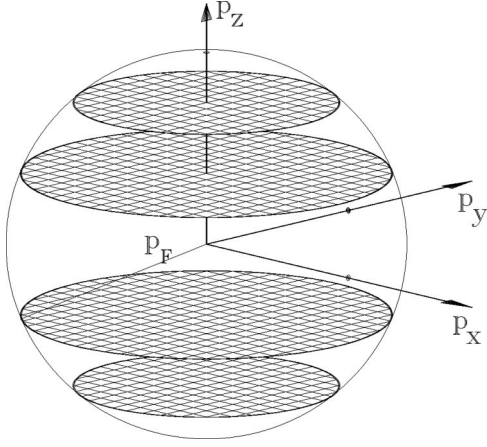


FIG. 1. Population of nucleonic momentum space for *bulk* matter of an idealized sheet, infinite in  $x$ - $y$  dimensions. The  $z$  axis is perpendicular to the surface of the sheet.

$$f(\mathbf{p}, z) = \frac{4\Delta p_z}{h^3} \sum_{k=1}^{\infty} \delta(p_z \pm \sqrt{k^2 \Delta p_z^2 - S(z)}). \quad (2)$$

Here  $\delta()$  denotes the Dirac delta function, the factor 4 represents the spin-isospin degeneracy, and the function  $S(z)$  describes the  $z$  dependence of the momentum-independent part of the effective single-nucleon potential

$$S(z) = \text{mod} \left( U(z) - U(0), \frac{\Delta p_z^2}{2M} \right), \quad (3)$$

where  $M$  denotes the average nucleon mass (taken as  $M = 938.903 \text{ MeV}/c^2$ ). The origin of the  $z$  coordinate is set half way between the sheet surfaces. A boldface font is used in Eq. (2) and throughout this paper to denote a vector quantity.

For the nuclear matter density  $\rho(z)$ , the single-particle potential  $U(\mathbf{p}, z)$ , and the energy per nucleon  $\epsilon_V(z)$ , one writes then in a close analogy to Refs. [9–12]

$$\rho(z) = \int_{FS(z)} d\mathbf{p} f(\mathbf{p}, z), \quad (4)$$

$$U(\mathbf{p}, z) = \int d\mathbf{r}' \int_{FS(z)} d\mathbf{p}' f(\mathbf{p}', z) V(|\mathbf{r} - \mathbf{r}'|, |\mathbf{p} - \mathbf{p}'|), \quad (5)$$

and

$$\epsilon_V(z) = \frac{1}{\rho(z)} \int_{FS(z)} d\mathbf{p} f(\mathbf{p}, z) \left[ \frac{p^2}{2M} + \frac{1}{2} U(\mathbf{p}, z) \right], \quad (6)$$

respectively. In the above equations,  $V(r, p)$  denotes the nucleon-nucleon interaction, and  $\int d\mathbf{r}$  and  $\int_{FS(z)} d\mathbf{p}$  denote integration over the (infinite) nuclear volume and over the Fermi sphere of a radius  $p_F(z)$  in momentum space, respectively. Assuming that the range of the nucleon-nucleon interaction is small compared to the linear dimensions of the *bulk* domain, the spatial integration in Eq. (5) is effectively limited to this domain. Then, for the *bulk* matter of interest here,

all quantities in Eqs. (2)–(6) are  $z$  independent, in agreement with the definition of the *bulk* matter.

The nucleon-nucleon interaction was assumed to be momentum dependent and given by the Seyler-Blanchard [9] formula

$$V(r, p) = -C \frac{e^{-r/a}}{(r/a)} \left( 1 - \frac{p^2}{b^2} \right), \quad (7)$$

where  $C$  represents the strength of the interaction, the parameter  $a$  represents the range of the Yukawa force, and  $b$  denotes a critical value of the relative momentum, beyond which the force becomes repulsive. The quantities  $r$  and  $p$  are the distance between the nucleons and their relative momentum, respectively. Values of the parameters of the interaction were taken to be equal to [10]  $C = 328.61 \text{ MeV}$ ,  $a = 0.62567 \text{ fm}$ , and  $b = 392.48 \text{ MeV}/c$ . For infinite symmetric nuclear matter [10], these values assure a volume energy per nucleon of  $\epsilon_V = -15.677 \text{ MeV}$  and a kinetic Fermi energy of  $33.138 \text{ MeV}$ .

A straightforward analytical integration in Eqs. (4), (5), and (6), using Eq (7), yields for the *bulk* matter (the  $z$  argument is left out for the sake of brevity)

$$\rho = \frac{8\pi}{h^3} \left( p_{zF} p_F^2 - \frac{1}{3} p_{zF}^3 - \frac{1}{2} \Delta p_z p_{zF}^2 \right) - \frac{1}{6} (\Delta p_z)^2 p_{zF}, \quad (8)$$

$$U(p) = V_o + V_1 \frac{p^2}{b^2}, \quad (9)$$

and

$$\epsilon_V = -\frac{1}{2} V_1 + \epsilon_T \frac{M}{M_{eff}}. \quad (10)$$

Here,

$$\epsilon_T = \frac{2\pi}{h^3 \rho M} \left( p_{zF} p_F^4 - \frac{1}{5} p_{zF}^5 - \frac{1}{2} \Delta p_z p_{zF}^4 \right) - \frac{1}{3} (\Delta p_z)^2 p_{zF}^3 + \frac{1}{30} (\Delta p_z)^4 p_{zF} \quad (11)$$

is the average kinetic energy of a nucleon and

$$M_{eff} = M \frac{b^2}{b^2 + 2M V_1} \quad (12)$$

is the effective mass summarizing effects of the interaction component quadratic in nucleonic momentum  $p$ . The strengths of the momentum-dependent and momentum-independent components of the effective single-nucleon potential, respectively, are given by

$$V_1 = 4\pi C a^3 \rho \quad (13)$$

and

$$V_o = -V_1 \left( 1 - \frac{2M}{b^2} \epsilon_T \right). \quad (14)$$

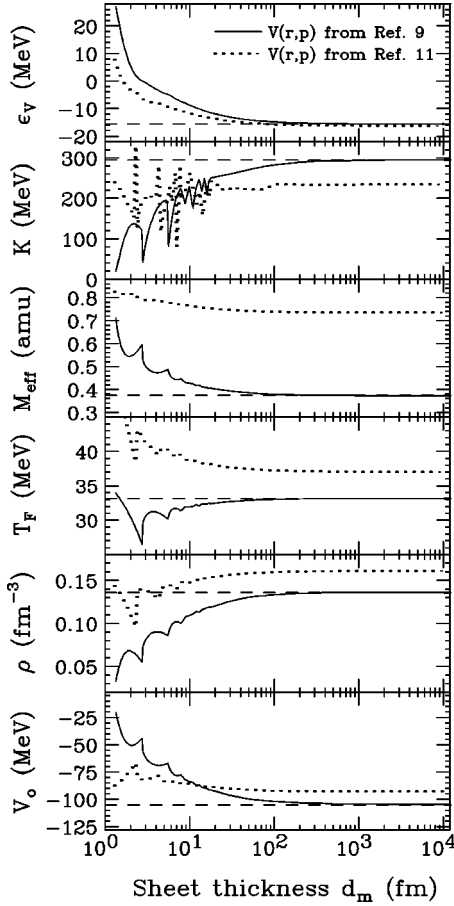


FIG. 2. From top to bottom: volume energy per nucleon, compressibility coefficient, reduced mass, nucleon kinetic Fermi energy, matter density, and strength of the momentum-independent single-particle potential, as functions of the sheet thickness  $d_m$ . The solid curves are obtained with the Seyler-Blanchard (Ref. [8]) nucleon-nucleon interaction parametrization with values of the parameters as indicated in the legend. Results obtained with the parametrization of the interaction as proposed in Ref. [11] are shown with dotted lines.

The quantity  $p_{zF}$  in Eqs. (8) and (11) denotes the maximum value of the perpendicular momentum  $p_z$  allowed for a given Fermi momentum  $p_F$

$$p_{zF} = p_F - \text{mod}(p_F, \Delta p_z). \quad (15)$$

Note that the corresponding equations for infinite nuclear matter, characterized by a uniform population function  $f(\mathbf{p}, z) = 4/h^3$ , can be readily obtained from the above Eqs. (8)–(13) by setting  $p_{zF} = p_F$ , while dropping all terms containing powers of  $\Delta p_z$ .

The quantity of interest in the present study is the minimum value of the energy per nucleon,  $\epsilon_V$ , for *bulk* nuclear matter confined to the geometry of a sheet of finite thickness. This value can be obtained by varying the input value of the Fermi momentum  $p_F$  in a search routine minimizing  $\epsilon_V$ . Note that a calculation of  $\epsilon_V$  for given  $p_F$  and  $d$  entails the use of Eqs. (1), (15), (8), (13), (11), (12), and (10) in an ordered sequence. Note also that in the above equations, momenta are expressed in units of MeV/c, energies in units of

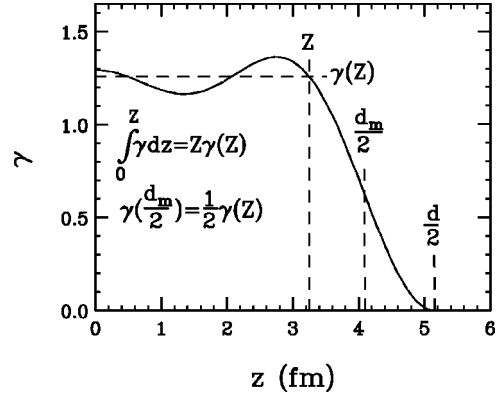


FIG. 3. The relationship between the *model* and the *matter* thickness of a sheet of nuclear matter.

MeV, lengths in units of femtometer, and masses in units of MeV/c<sup>2</sup>. Accordingly, the Planck constant is in units of MeV fm/c,  $h = 1239.86$  MeV fm/c.

Results of the calculations are summarized in Fig. 2, where values of selected parameters characterizing properties of the *bulk* sheet matter are plotted vs the *matter* thickness  $d_m$  of the sheet. The latter quantity was evaluated for any given *model* thickness  $d$  based on the idealized matter density profile  $\gamma(z)$  along the direction perpendicular to the sheet surface. The procedure of evaluating  $d_m$  is illustrated in Fig. 3. The density profile of interest was generated by (weighted) summing of the  $\sin^2[2\pi(z-d/2)p_z/h]$  functions for the actual distribution of  $p_z$ . The quantity  $d_m$  was defined via the requirement that the density  $\gamma(d_m/2)$  be equal to one-half of the bulk density  $\gamma_b$ , where the latter was defined via the “outermost” (i.e., highest in  $z < d/2$ ) solution of the equation

$$\int_0^Z \gamma(z) dz = Z \gamma(Z) = Z \gamma_b. \quad (16)$$

The difference between the *model* and *matter* thicknesses calculated in the above manner depends on  $d$ . It increases linearly from 0 to its maximum value of approximately 2.8 fm, with  $d$  increasing from 0 to 5.6 fm. For  $d > 5.6$  fm, this difference decreases quasihyperbolically with thickness, reaching saturation at approximately 2 fm for  $d > 20$  fm.

The main result of the present study is displayed in the top panel of Fig. 2. As seen in this panel, the maximum possible binding energy per nucleon decreases dramatically as the thickness  $d_m$  of the sheet decreases. This energy becomes negative, i.e.,  $\epsilon_V$  becomes positive and the system becomes unbound for thicknesses of about  $d_m \approx 2.8$  fm and below ( $d < 5.6$  fm). This effect of an increase in energy per nucleon with decreasing thickness of the sheet results purely from the quantization of the perpendicular component  $p_z$  of the momentum [see Eq. (2)].

This feature is only approximately accounted for by the standard droplet-model formula relying on a uniform, Thomas-Fermi population of the Fermi sphere in momentum space. The latter model “adjusts” the parameters of the effective nucleon-nucleon interaction to have the average shell

effects included in the surface energy term. The model relies here on the fact that for compact shapes (e.g., of a square box) the integrated (over the nuclear volume) shell effect is to a good approximation proportional to the surface area. The latter proportionality is due to the fact that the average shell correction to the volume energy arising from a confinement in any particular direction is inversely proportional to the confinement width (here, thickness of the sheet) in this direction. When multiplied by volume, this correction becomes proportional to the associated surface area. Adding the corrections for confinements in all three directions  $x$ ,  $y$ , and  $z$  results, thus, in an overall quantum correction term proportional to the total surface area.

The large magnitude of the volume shell effect raises the question whether the standard droplet model accounts accurately for these effects in the cases of exotic shapes and whether it is, therefore, applicable at all to nuclear matter in noncompact geometries. The present paper does not answer this question fully. At any rate, this *quantum* effect is largely responsible for the resistance of nuclear matter against the development of noncompact geometries associated with exotic spatial confinements of nucleonic motion, in addition to that generated by a “true” surface tension. It gives rise to strong effective forces, akin to repulsive diabatic forces [15], driving the nuclear system away from a formation of noncompact shapes attained dynamically in nuclear reactions.

From the top panel of Fig. 2, one notes that the value of the energy per nucleon for the *bulk* sheet matter differs significantly from the asymptotic value of  $\epsilon_{V\infty} = -15.7$  MeV already for sheet thicknesses  $d_m$  comparable in magnitude to nuclear diameters. This indicates that the parameters of the Seyler-Blanchard interaction [9,10] are not well suited for absolute, more accurate calculations of the type reported in the present work. The same is true with respect to any parametrization that is set up to describe average trends in nuclear masses and, hence, accounts for the average shell effects due to a particular shape of a sphere, but not those associated with arbitrary shapes.

For comparison in Fig. 2, results obtained with a recently proposed [11,12] parametrization of the nucleon-nucleon interaction are shown as dotted lines. This new parametrization adds two terms to the Seyler-Blanchard form—an attractive interaction inversely proportional to the relative momentum, and a repulsive component proportional to the two-thirds power of the nuclear matter density. The integrals involving the former term were evaluated numerically. It is clear from the top panel of Fig. 2 that, although the quantum effect discussed above depends on the nucleon-nucleon interaction, it is strong for either [10–12] parametrization. The large increase of  $\epsilon_V$  with decreasing sheet thickness suggests a strong resistance of nuclear matter against such deformation.

The remaining four panels of Fig. 2, shown mostly for the sake of completeness, illustrate effects of a quantization of the perpendicular momentum  $p_z$  on selected properties of nuclear matter at the stationary density minimizing the energy per nucleon of *bulk* matter. Sharp dips and peaks in the respective functions result from the discontinuities in first derivatives of the underlying momentum distribution at values of momenta  $p$  that are integer multiples of the elementary quantum  $\Delta p_z$ . One notes, that the new parametrization [11,12] results in asymptotic values of the parameters that are different from those obtained using the “old” [10] parametrization, in agreement with those reported in Ref. [12]. In particular, the values of effective masses obtained with the new parametrization appear much more realistic.

In conclusion, the present analysis demonstrates the importance of quantum effects for noncompact nuclear shapes. These effects are shown to generate a pressure offering resistance of the nuclear systems against the development of noncompact geometries and to generate forces driving these systems toward compact shapes. The large magnitude of the effects discussed above allows one to question the validity of the approximation made in the standard liquid-drop model in cases of extreme noncompact geometries, sometimes considered in the literature. It allows one also to question the validity of BUU type of computations in cases where noncompact geometries are involved. One notes in this latter respect that, similarly to the Thomas-Fermi method discussed in this study, the BUU equations do not consider effects of spatial confinement on the spectrum of allowed states in momentum space. While it is not clear, to what extent semiclassical models such as the modified Thomas-Fermi approach followed in the present work, can capture the essential features of strongly quantized systems, more accurate calculations, including surface and Coulomb energies, as well as effects of a finite nuclear temperature seem desirable. A thorough investigation of the implications of the findings made in the present work for several issues, appear clearly warranted. Problems of high relevance to current reaction studies include questions to the validity of BUU and other types of calculations, as well as issues associated with the magnitude of realistic droplet-model parameters for nuclear matter, in general, and not only for the specific case of spherical geometries of real nuclei. For example, of relevance in this context are issues concerning the relative stability of the neck matter between the interacting nuclei and the decay modes of nuclear matter. This problem is especially interesting for an understanding of the dynamical production of intermediate-mass fragments [16] in heavy-ion reactions.

Illuminating discussions with Dr. W. J. Swiatecki are gratefully acknowledged. This work was supported by the U.S. Department of Energy Grant No. DE-FG02-88ER40414.

[1] C. Wong, *Ann. Phys. (N.Y.)* **77**, 279 (1973).

[2] W. Bauer, G. Bertsch, and H. Schultz, *Phys. Rev. Lett.* **69**, 1888 (1992).

[3] L. Moretto, K. Tso, N. Colonna, and G. Wozniak, *Phys. Rev.*

*Lett.* **69**, 1884 (1992).

[4] L. Moretto and G. Wozniak, *Annu. Rev. Nucl. Part. Sci.* **379**, (1993).

[5] B. Borderie, B. Remaud, M. Rivet, and F. Sebille, *Phys. Lett.*

- B **302**, 15 (1993); **307**, 404(E) (1993).
- [6] G. Batko and J. Randrup, Nucl. Phys. A **563**, 97 (1993).
- [7] H. Xu, C. Gagliardi, R. Tribble, and C. Wong, Phys. Rev. C **49**, 1778 (1994).
- [8] L. Moretto, K. Tso, and G. Wozniak, Phys. Rev. Lett. **78**, 824 (1997).
- [9] R. Seyler and C. Blanchard, Phys. Rev. **124**, 227 (1963); **131**, 355 (1967).
- [10] W. Myers and W. Swiatecki, Ann. Phys. (N.Y.) **55**, 395 (1990).
- [11] W. Myers and W. Swiatecki, Ann. Phys. (N.Y.) **204**, 401 (1990); **211**, 292 (1990).
- [12] W. Myers and W. Swiatecki, Nucl. Phys. **A601**, 141 (1996).
- [13] G. Bertsch, H. Kruse, and S.D. Gupta, Phys. Rev. C **29**, 673 (1984); G.F. Bertsch and S. Das Gupta, Phys. Rep. **160**, 189 (1988).
- [14] C. Gregoire *et al.*, Nucl. Phys. **A465**, 317 (1987).
- [15] W. Nörenberg, Phys. Lett. **104B**, 107 (1981).
- [16] J. Töke *et al.*, Phys. Rev. Lett. **77**, 3514 (1996).